

Probing semiconductor quantum dot state and manipulation with superconducting transmission line resonator

Zhe Guan*

Department of Physics, University of Science and Technology of China, Hefei 230026, People's Republic of China

(Dated: June 15, 2013)

A coupled system of a superconducting transmission line resonator with a semiconductor double quantum dot is analyzed. We simulate the phase shift of the microwave signal in the resonator, which is sensitive to the quantum dot qubit state and manipulation. The measurement quality is sufficiently high and the results demonstrate a solid-state quantum processor based on this type of circuit can be envisioned.

PACS numbers: 03.67.-a,73.63.Kv

The interaction between light and matter has been a major focus of research in atomic physics and quantum optics for a long time [1]. There were many significant advances in the realization of quantum phenomena in manipulating atoms and photons to demonstrate elementary aspects of quantum physics[2–5]. The most fundamental form of this kind of interaction is that a single photon interacts with a single atom. With the generation of cavity quantum electrodynamics, coherent quantum Rabi oscillations between the atom and the cavity has been experimentally observed using Rydberg atoms in microwave cavities [4, 6] and alkali atoms in optical cavities [7]. Developments have been made in replacing the natural atoms with artificial two-level systems in solid-state systems, such as the superconducting quantum bits (qubits) [8–10]. Recently, a semiconductor double quantum dot (DQD) coupled with electromagnetic field of a superconducting microwave resonator has been experimentally realized [11–13]. Especially, the observed distinct vacuum Rabi splitting indicates that a strong coupling exists in this system [12]. By introducing the architecture of circuit quantum electrodynamics (cQED), this semiconductor-superconductor hybrid system shows the advantage of scalability to coherently couple qubits and resonators on one chip compared to other systems. Furthermore, the coupled system has been applied to spin dynamics[13]. These works have paved a way for fast quantum information processing in semiconductor structures, which would be rather useful in quantum computing and quantum communication. Here we demonstrate how to probe the DQD state and manipulation using the superconducting transmission line resonator, exploiting the potential of the resonator as 'quantum detector' of the qubit.

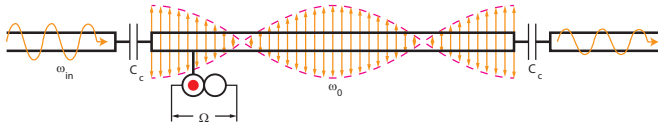


FIG. 1. The GaAs/AlGaAs semiconductor double quantum dot is coupled to the superconducting transmission line resonator via capacitive coupling, and a continuous microwave is induced to the transmission line from the left side.

The schematic diagram of the capacitive coupled system of GaAs/AlGaAs semiconductor DQD and superconducting transmission line resonator, is shown in Fig. 1. Jaynes-Cummings Hamiltonian can be used to describe the whole system under the rotating-wave approximation [11]:

$$\hat{H}_0 = \frac{\hbar\Omega}{2}\hat{\sigma}_z + \hbar\omega_0(\hat{a}^\dagger\hat{a} + \frac{1}{2}) + \hbar g(\hat{\sigma}_+\hat{a} + \hat{\sigma}_-\hat{a}^\dagger), \quad (1)$$

$$\Omega = \sqrt{\varepsilon^2 + 4t^2}$$

Here $\hat{\sigma}_z$, $\hat{\sigma}_+$, $\hat{\sigma}_-$ are the Pauli operators in the basis of $|\uparrow\rangle$ (qubit excited state) and $|\downarrow\rangle$ (qubit ground state) of the DQD, a and a^\dagger are the annihilation and creation operators of the photon in the resonator respectively, and ω_0 is the bare frequency of the resonator. ε is the detuning energy between the charge qubit states, t is the inter-dot tunneling rate, and g is the coupling strength between the DQD and the resonator.

Currently research on this system focuses on the dispersive region [11, 13]. To realize probing the DQD state using the superconducting transmission line, we can simulate the time-evolution of the density matrix of the coupled system, with the transmission line imposed by a continuous microwave field. We use the standard master-equation method with a Markovian approximation [11]:

$$\frac{d\rho}{dt} = \frac{i}{\hbar}[\rho, \hat{H}_0] - \frac{\kappa}{2}(\hat{a}^\dagger\hat{a}\rho - 2\hat{a}\hat{a}^\dagger\rho + \rho\hat{a}^\dagger\hat{a}) - \frac{\gamma_l}{2}(\hat{\sigma}_-\hat{\sigma}_+\rho - 2\hat{\sigma}_-\rho\hat{\sigma}_+ + \rho\hat{\sigma}_-\hat{\sigma}_+) - \frac{\gamma_\phi}{2}(\rho - \hat{\sigma}_z\rho\hat{\sigma}_z + \rho) \quad (2)$$

Here ρ is the density matrix of the coupled system, κ is the decay rate of the resonator, γ_l is the energy relaxation rate, γ_ϕ is the dephasing rate, ω_0 is the frequency of the resonator. When the DQD is near the

* guanz@mail.ustc.edu.cn

inter-dot charge transitions ($\varepsilon = 0$), the energy of the DQD is close to the microwave field energy, allowing a more effective photon exchange between the DQD and the microwave field. The strengthened exchange results in a phase shift of the microwave imposed in the transmission line. To calculate the phase shift under various circumstances of the coupled system, we use $\phi = \arg(i \langle \hat{a} \rangle)$ as the phase response [14, 15]. In the Shrödinger picture, we could easily extract the phase shift of the microwave after we simulate the time-evolution of the density matrix of the coupled system. Especially, we have the phase shift $\Delta\phi = -\arctan(2g^2/\kappa\Delta)$ when $\Delta > g$.

In Fig. 2, the numerical simulation of phase shift $\Delta\phi$ of the microwave is plotted as a function of ε and $2t$ of the DQD, with $2t/\hbar$ ranging from 0 to 20 GHz and ε/\hbar ranging from -20 to 20 GHz. Here we use the realistic parameters in the experiments as $\omega_0/2\pi = 6.2$ GHz, $\kappa/2\pi = 3.1$ MHz, $\gamma = 66.7$ MHz, $\gamma_\phi = 0$ MHz [11–13]. Sign change of the DQD-transmission line detuning, Δ at different value of ε introduces the sign change of $\Delta\phi$. Along the $2t$ axis at a fixed ε , there is a sharp increment of $\Delta\phi$ from negative to positive near $2t/\hbar = 6.2$ GHz, which could be clearly observed in the 3D plot of phase shift distribution in the $\varepsilon - 2t$ plane. From this picture, we can conclude that the DQD spectroscopy can be efficiently probed by the coupled transmission line resonator.

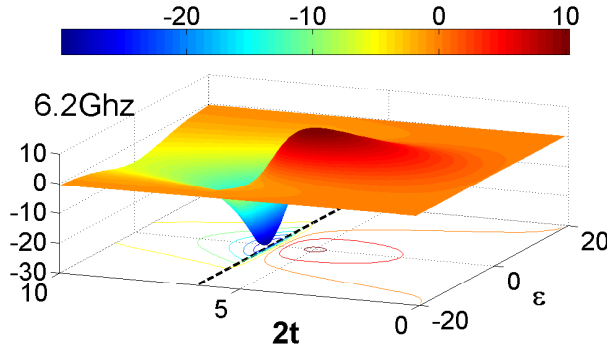


FIG. 2. The phase shift $\Delta\phi$ of the microwave is depicted as the function of ε and $2t$. In the $\varepsilon - 2t$ plane, the density of isolines when $2t/\hbar$ is near 6.2 GHz is much bigger than other part of the plane, illustrating the sharp increment of $\Delta\phi$.

We can also probe the manipulation process of the semiconductor DQD by reading out the phase shift of the microwave. In this scheme, an operation pulse is applied to the DQD as illustrated in Fig. 3a [16]. The DQD initially stays at its charge state $|R\rangle$. Due to the employed short pulse, the DQD will be driven to the charge degeneracy point nonadiabatically. Since $|R\rangle$ is no longer an eigenstate, the DQD starts to evolve during the pulse duration time t_p . When the pulse is terminated, the DQD stays in the superposition of $|R\rangle$ and $|L\rangle$ states. After the manipulation pulse is applied to the DQD, the energy relaxation of the qubit exists and we conduct continuous

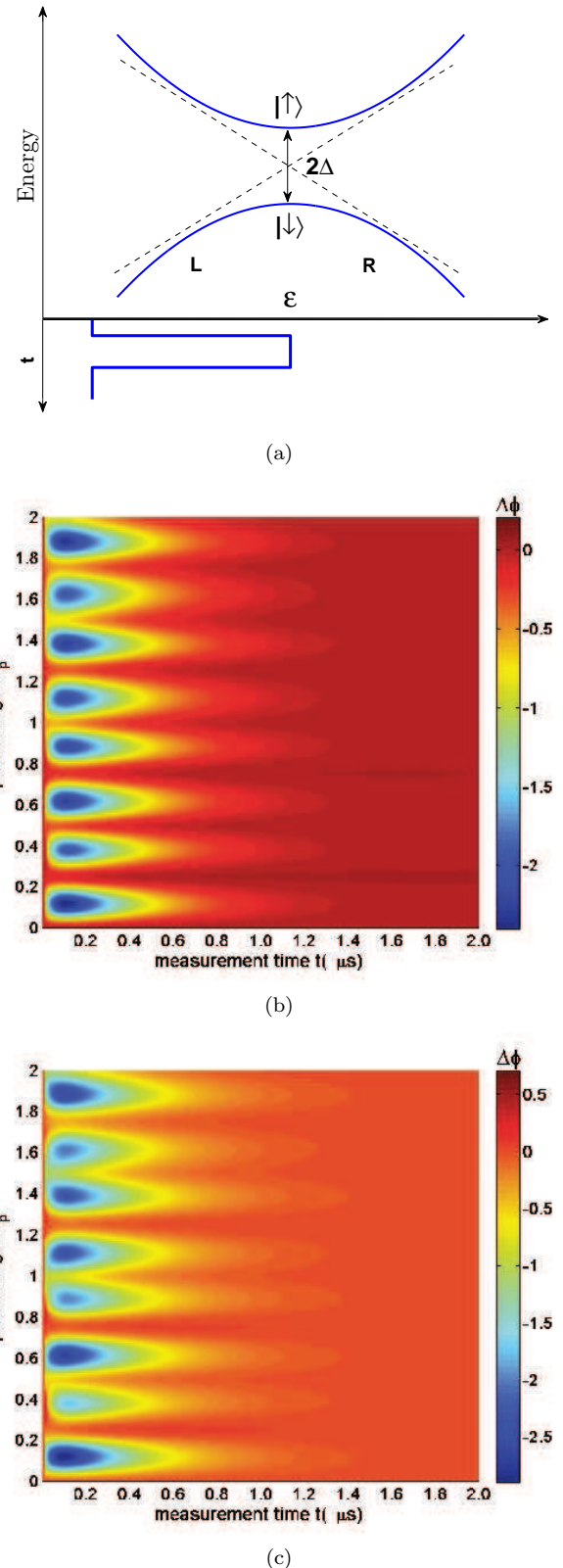


FIG. 3. (a) Schematic of the charge qubit energy level diagram with a short rectangle driven pulse. (b) The phase shift $\Delta\phi$ of the microwave resonator is depicted as a function of measurement time t and pulse length t_p . The photon number in the resonator is 3.8. A clear qubit Rabi oscillation pattern with little deviation is obtained in the phase shift domain. (c) When the photon in the resonator is 0.6, the less frequency modes would increase the disturbing effect on the original manipulation frequency, which induces a larger deviation from perfect Rabi oscillation pattern.

monition of the resulted phase shift of the resonator.

In Fig. 3b and 3c, we plot the phase shift $\Delta\phi$ as a function of measurement time t and pulse length t_p with different amplitudes of the induced microwave. Here we use the realistic parameters as $\omega_0/2\pi = 6.2$ GHz, $\kappa/2\pi = 1$ MHz, $\gamma_1 = 20$ MHz, $\gamma_\phi = 200$ MHz [11–13]. In Fig. 3b, the steady photon number in the resonator is 3.8, we can see that when apply a short rectangle pulse to manipulate the DQD, we can obtain a clear periodical Rabi oscillation pattern of the phase shift. Before the pulse is applied, the phase shift has a minimum value which is approximately 0 corresponding to the initial state of the qubit. When $t_p = 0.1$ ns, we have the maximum phase shift of -2.4 deg, and this is because the qubit has been pulled to its superposed state due to the induced pulse. On the contrary, when $t_p = 0.3$ ns, no phase shift is observed since the qubit remains its initial state under the pulse. Also the phase shift response to the $t_p = 0.1$ ns pulse is almost the same with that to the $t_p = 0.6$ ns pulse, and this is due to that the time scale of Rabi oscillation is much shorter than the energy relaxation time of the qubit. Additionally, since the qubit would decay from its excited state to the ground state exponentially with the relaxation time $T_1 = 1/\gamma$, the phase shift would also decay as the measurement time t extends, and it is observable that after $t = 0.7$ μ s, hardly we can monitor any phase shift even though a pulse is applied on the qubit. Also, we could obviously sense the phenomenon that the phase shift Rabi oscillation pattern is not perfectly pe-

riodic. The reason lies in that our manipulation pulse length is small thus the disturbance from other frequency modes besides the manipulation frequency is comparably notable, which results in the deviation from periodicity. The deviation is more serious in Fig. 3c where the steady photon number in the resonator is 0.6, which means the frequency modes in the system is less than that in Fig. 3b. The mix of more modes would decrease the disturbing effect, so it is not hard for us to understand the periodicity is worse in Fig. 3c. Overall, we have achieved probing the DQD manipulation by monitoring the phase shift of the microwave resonator.

In conclusion, we have comprehensively analyzed and simulated the phase shift in microwave transmission line, which could help us probe the state of the DQD. Additionally, by monitoring the phase shift of the microwave transmitted in the line, we could probe our operation on the DQD. Our work paves a way to possible applications using the resonator as the highly efficient detector which would be attractive to the further quantum information processing.

This work was supported by the National Basic Research Program of China (Grant No. 2011CB921200), the CAS, the National Natural Science Foundation of China (Grant Nos. 11274289 and 11105135), the Fundamental Research Funds for the Central Universities (Nos. WK2470000011). ZG acknowledges support from the Fund for Fostering Talents in Basic Science of the National Natural Science Foundation of China (No. J1103207).

[1] M. O. Scully, and M. S. Zubairy, *Quatum Optics*. *Cambridge University Press*, (1997).

[2] J. C. Bergquist, R. G. Hulet, W. M. Itano, and D. J. Wineland, Observation of Quantum Jumps in a Single Atom. *Phys. Rev. Lett.* **57**, 1699 (1986).

[3] C. Monroe, D. M. Meekhof, B. E. King, W. M. Itano, and D. J. Wineland, Demonstration of a fundamental quantum logic gate. *Phys. Rev. Lett.* **75**, 4714 (1995).

[4] M. Brune, F. Schmidt-Kaler, A. Maali, J. Dreyer, E. Hagley, J. M. Raimond, and S. Haroche, Quantum Rabi Oscillation: A Direct Test of Field Quantization in a Cavity. *Phys. Rev. Lett.* **76**, 1800 (1996).

[5] M. Brune, S. Haroche, J. M. Raimond, L. Davidovich, and N. Zagury, Manipulation of photons in a cavity by dispersive atom-field coupling: Quantum-nondemolition measurements and generation of “Schrödinger cat” states. *Phys. Rev. A* **45**, 5193 (1992).

[6] J. Raimond, M. Brune, and S. Haroche, Manipulating quantum entanglement with atoms and photons in a cavity. *Rev. Mod. Phys.* **73**, 565 (2001).

[7] R. J. Thompson, G. Rempe, and H. J. Kimble, Observation of normal-mode splitting for an atom in an optical cavity. *Phys. Rev. Lett.* **68**, 1132 (1992).

[8] J. M. Martinis, S. Nam, J. Aumentado, and C. Urbina, Rabi oscillations in a large Josephson-junction qubit. *Phys. Rev. Lett.* **89**, 117901 (2002).

[9] T. Yamamoto, Y. A. Pashkin, O. Astafiev, Y. Nakamura, and J. S. Tsai, Demonstration of conditional gate operation using superconducting charge qubits. *Nature* **425**, 941 (2003).

[10] A. Wallraff, D. I. Schuster, A. Blais, L. Frunzio, R. S. Huang, J. Majer, S. Kumar, S. M. Girvin, and R. J. Schoelkopf, Strong coupling of a single photon to a superconducting qubit using circuit quantum electrodynamics. *Nature* **431**, 162 (2004).

[11] T. Frey, P. J. Leek, M. Beck, A. Blais, T. Ihn, K. Ensslin, and A. Wallraff, Dipole Coupling of a Double Quantum Dot to a Microwave Resonator. *Phys. Rev. Lett.* **108**, 046807 (2012).

[12] H. Toida, T. Nakajima, and S. Komiyama, Circuit QED using a semiconductor double quantum dot. *arXiv* **1206**, 0674v1 (2012).

[13] D. Petersson, L. W. McFaul, M. D. Schroer, M. Jung, J. M. Taylor, A. A. Houck, and J. R. Petta, Circuit quantum electrodynamics with a spin qubit. *Nature* **490**, 380 (2012).

[14] A. Wallraff, D. I. Schuster, A. Blais, L. Frunzio, J. Majer, M. H. Devoret, S. M. Girvin, and R. J. Schoelkopf, Approaching Unit Visibility for Control of a Superconducting Qubit with Dispersive Readout. *Phys. Rev. Lett.* **95**, 060501 (2005).

[15] Alexandre Blais, Ren-Shou Huang, Andreas Wallraff, S. M. Girvin, and R. J. Schoelkopf, Cavity quantum electrodynamics for superconducting electrical circuits: An

architechture for quantum computation. *Phys. Rev. A.* **69**, 062320 (2004).

[16] K. D. Petersson, J. R. Petta, H. Lu, and A. C. Gossard, Quantum Coherence in a One-Electron Semiconductor Charge Qubit. *Phys. Rev. Lett.* **105**, 246804 (2010).